Acta Crystallographica Section F
Structural Biology and Crystallization Communications
ISSN 1744-3091

Crystallization and preliminary crystallographic analysis of Gre2p, an NADP$^+$-dependent alcohol dehydrogenase from *Saccharomyces cerevisiae*

Klaus Breicha,[a]‡ Marion Müller,[b]‡ Werner Hummel[b]* and Karsten Niefind[a]*

[a]Institut für Biochemie, Department für Chemie, Universität zu Köln, Zülpicher Strasse 47, D-50674 Köln, Germany, and [b]Institut für Molekulare Enzymtechnologie, Heinrich-Heine Universität Düsseldorf im Forschungszentrum Jülich, D-52426 Jülich, Germany

‡ These authors contributed equally to this work.

Correspondence e-mail: w.hummel@fz-juelich.de, karsten.niefind@uni-koeln.de

Received 21 April 2010
Accepted 20 May 2010

Gre2p [**G**enes de **r**espuesta a **e**stres (stress-response gene)] from *Saccharomyces cerevisiae* is a monomeric enzyme of 342 amino acids with a molecular weight of 38.1 kDa. The enzyme catalyses both the stereospecific reduction of keto compounds and the oxidation of various hydroxy compounds and alcohols by the simultaneous consumption of the cofactor NADPH and formation of NADP$^+$. Crystals of a Gre2p complex with NADP$^+$ were grown using PEG 8000 as a precipitant. They belong to the monoclinic space group $P2_1$. The current diffraction resolution is 3.2 Å. In spite of the monomeric nature of Gre2p in solution, packing and self-rotation calculations revealed the existence of two Gre2p protomers per asymmetric unit related by a twofold noncrystallographic axis.

1. Introduction

The alcohol dehydrogenase Gre2p from *Saccharomyces cerevisiae* has been shown to be a versatile biocatalyst for the synthesis of enantiopure hydroxy compounds, which serve as valuable building blocks for the production of a variety of pharmaceuticals and fine chemicals (Müller *et al.*, 2010; Choi *et al.*, 2010; Ema *et al.*, 2008). The enzyme has a monomeric structure and is predominately NADPH-dependent. Its substrate spectrum is very comprehensive: Gre2p catalyses the reduction of various diketones, α-keto and β-keto esters, aliphatic and aromatic aldehydes as well as some aliphatic ketones and hydroxy ketones (Müller *et al.*, 2010; Kaluzna *et al.*, 2002; Ema *et al.*, 2001).

Although the enzyme has been characterized well in terms of its applicability for stereoselective and enantioselective asymmetric synthesis, only scarce information is known about its physiological function. Analysis of the *S. cerevisiae* proteins induced by several stress stimuli revealed that the transcription level of the Gre2p-encoding gene is increased, suggesting a role of the enzyme in the stress-response system (Hauser *et al.*, 2007; Vido *et al.*, 2001; Garay-Arroyo & Covarrubias, 1999). This finding led to the designation '**G**enes de **r**espuesta a **e**stres' (stress-responsive gene).

Further studies have proposed Gre2p to be part of the detoxification of methylglyoxal in the cell, naming the *GRE2* gene product as a methylglyoxal reductase (EC 1.1.1.283; Chen *et al.*, 2003), and to be a suppressor of isoamyl alcohol-induced filament formation, suggesting that *GRE2* encodes an isovaleraldehyde reductase (EC 1.1.1.265; Hauser *et al.*, 2007). In addition to this, Warringer & Blomberg (2006) demonstrated Gre2p to be involved in yeast ergosterol biosynthesis, as *gre2*-Δ deletion strains displayed several growth defects during environmental stress, *e.g.* using the Ca^{2+} chelator ethylene glycol tetraacetic acid (EGTA), which decreases the intracellular Ca^{2+} concentration. Additionally, these strains revealed sensitivity to ergosterol-inhibiting enzymes.

The primary sequence of the enzyme comprises 342 amino acids, possesses the typical cofactor-binding motif (Rossmann fold) at the N-terminus and exhibits an indispensable catalytic triad (Filling *et al.*, 2002) composed of Ser126–Tyr165–Lys169. Thus, Gre2p can be grouped into the extended short-chain dehydrogenase/reductase superfamily according to Persson *et al.* (2009) and Jörnvall *et al.*

(1995). Moreover, Gre2p has sequence similarity to dihydroflavonol reductases from higher plants (Casamayor *et al.*, 1995), *e.g.* that from *Vitis vinifera*, and is a distant homologue of mammalian 3-β-hydroxysteroid dehydrogenases (Warringer & Blomberg, 2006), *e.g.* those from mouse and rat. The highest homology to a protein of solved three-dimensional structure is to aldehyde reductase II from the red yeast *Sporobolomyces salmonicolor*, with 30% identity (Kamitori *et al.*, 2005).

Three-dimensional structures of Gre2p in various functional states could provide useful insight into the substrate spectrum of the enzyme; they would be helpful for the application of Gre2p as a biocatalyst and in obtaining further information about its biological function in *S. cerevisiae*. Therefore, we were encouraged to crystallize the enzyme as the first step towards solving its structure.

2. Materials and methods

2.1. Protein preparation

The *GRE2* gene was cloned (Müller *et al.*, 2010), codon-optimized (unpublished results) and overexpressed in *Escherichia coli* BL21 (DE3). The resulting recombinant Gre2p protein was purified to homogeneity by three chromatographic separation steps (Müller *et al.*, 2010). Harvested cells (~6–7 g) were resuspended in 100 m*M* triethanolamine buffer (TEA) pH 7.0 containing 1 m*M* $MgCl_2$ at a ratio of 1 g cells (wet weight) to 2 ml buffer and were disrupted by three sonification cycles for 2 min (37% power output). Debris was removed by centrifugation under cooling at 45 000*g* for 30 min.

1.5 *M* ammonium sulfate was added to the crude extract and the suspension was incubated on ice for 2 h before precipitated protein was removed by centrifugation at 45 000*g* for 30 min at 277 K. The clear supernatant was loaded onto a Butyl Sepharose 4FF column (height 15 cm, diameter 1.6 cm; GE Healthcare) which had previously been equilibrated with 10 column volumes (CV) of 100 m*M* TEA buffer pH 7.0 containing 1 m*M* $MgCl_2$ and 1.5 *M* ammonium sulfate. After sample application, the column was washed for 2 h with the buffer at a flow rate of 1 ml min^{-1}. Elution of Gre2p was accomplished using the same buffer containing no ammonium sulfate with a linear gradient from 1.5 to 0 *M*.

Fractions were tested for their ability to reduce 2,5-hexanedione using the standard assay as described by Müller *et al.* (2010) and active fractions were pooled and loaded onto a Macro-Prep Ceramic Hydroxyapatite column (height 15 cm, diameter 1.6 cm; GE Healthcare) which had been equilibrated with 10 CV 5 m*M* potassium phosphate buffer (KP_i) pH 7.0 containing 1 m*M* $MgCl_2$, 150 m*M* NaCl. The enzyme was eluted with KP_i pH 7.0 containing 1 m*M* $MgCl_2$ using a linear gradient from 5 to 45 m*M*. The purification was carried out at a flow rate of 1 ml min^{-1}. Active fractions were pooled and loaded onto a HiLoad 16/60 Superdex 75 prep-grade column (GE Healthcare). This column was equilibrated with 10 CV 10 m*M* TEA buffer pH 6.8 and purification was accomplished at a flow rate of 1 ml min^{-1}. Samples obtained by this purification procedure had a purity of >95% as judged by SDS–PAGE analysis performed according to the method described by Laemmli (1970).

Prior to crystallization, the enzyme was concentrated using a Vivaspin 20 (30 kDa molecular-weight cutoff, Sartorius Stedim Biotech). The concentration of Gre2p was determined according to the method of Bradford (1976) using BSA as a standard. The final Gre2p concentration in the stock solution was 12 mg ml^{-1}.

Figure 1
Cocrystals of Gre2p and $NADP^+$ grown using PEG 8000 as a precipitant.

2.2. Crystallization

We attempted to grow crystals of both the apoenzyme and the complex with the cosubstrate $NADP^+$. All crystallization experiments were performed at 293 K with the sitting-drop variant of the vapour-diffusion method. For initial screening we used various sparse-matrix and grid screens from Hampton Research and from Jena Bioscience GmbH. Initial hits were optimized with additive screens also purchased from Hampton Research. The crystallization drops were pipetted on 96-well plates using a nanolitre dispenser (Hydra II from Matrix Technologies).

2.3. Diffraction data collection and analysis

Crystals were prepared for diffraction experiments under cryo-conditions by increasing the concentration of the precipitant (PEG 8000) in the mother liquor in two steps. Initially, half of the original reservoir solution [0.1 *M* 2-(*N*-morpholino)ethanesulfonic acid buffer (MES) pH 6.35, 15%(*w*/*v*) PEG 8000] was exchanged for 0.1 *M* MES buffer pH 6.35, 40%(*w*/*v*) PEG 8000; after mixing of the new reservoir solution re-equilibration occurred for 24 h. The reservoir solution was then completely exchanged for 0.1 *M* MES buffer pH 6.35, 40%(*w*/*v*) PEG 8000. After a new re-equilibration for at least 24 h the Gre2p crystals were flash-frozen in liquid nitrogen. X-ray diffraction data were collected on beamline BL14.2 of BESSY, Berlin using a MAR 224 CCD detector. The data-collection temperature was 100 K. The raw diffraction data were processed with *XDS* (Kabsch, 2010) and converted to structure-factor amplitudes using *TRUNCATE* from the *CCP*4 program suite (Collaborative Computational Project, Number 4, 1994).

2.4. Crystal-packing, Patterson and self-rotation function calculations

The Matthews coefficient (Matthews, 1968) and the solvent content were calculated with the program *MATTHEWS_COEF* (Collaborative Computational Project, Number 4, 1994). To look for possible pseudo-origin peaks generated by noncrystallographic translations a native Patterson function was computed using the program *FFT* from the *CCP*4 program suite (Collaborative Computational Project, Number 4, 1994). For a systematic search for noncrystallographic symmetry we used the program *GLRF* from the *REPLACE* package (Tong & Rossmann, 1997).

3. Results and discussion

After various crystal screening and optimization efforts the best crystals, judged according to the habitus (Fig. 1), grew to dimensions of up to 1.0 × 0.3 × 0.3 mm (Fig. 1) within two weeks. They were obtained from a Gre2p–$NADP^+$ solution prepared by mixing nine

parts of Gre2p stock solution and one part of 30 m*M* $NADP^+$ solution prior to crystallization. The reservoir solution consisted of 1 ml 0.1 *M* MES pH 6.35, 15%(*w*/*v*) PEG 8000. In the crystallization drop 5 µl of the Gre2p–$NADP^+$ mixture was added to 4 µl reservoir solution. The resulting solution was finally mixed with 0.5 µl 0.1 *M* cobalt chloride as an additive.

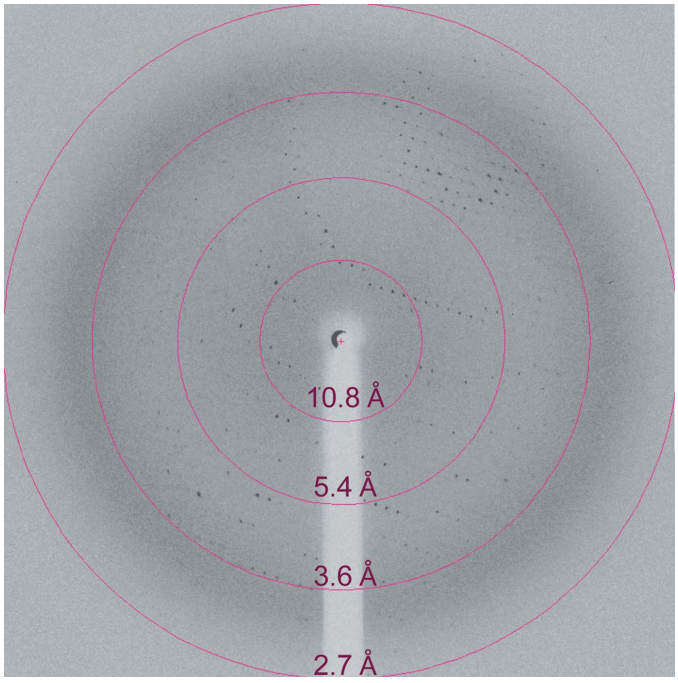

Figure 2
X-ray diffraction pattern of a monoclinic Gre2p–$NADP^+$ crystal with resolution rings.

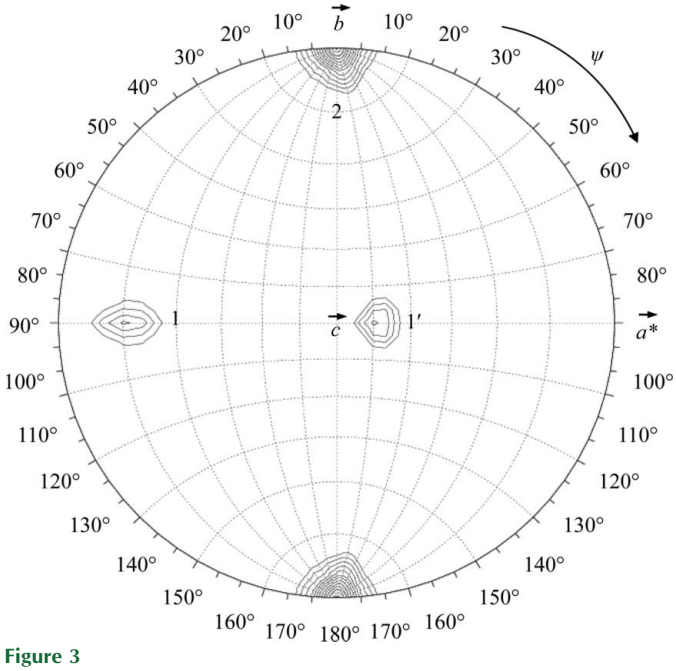

Figure 3
Section of the self-rotation function with $\kappa = 180^\circ$. The self-rotation function was calculated with *GLRF* (Tong & Rossmann, 1997) using diffraction data between 15 and 3.5 Å resolution. Contour lines are drawn starting from five r.m.s. (root-mean-square) deviations above the mean, in intervals of 0.5 r.m.s. deviations. The two peaks originating from the crystallographic twofold axis are labelled 2 and 2′, whereas the noncrystallographic peaks are designated 1 and 1′.

Table 1
Statistics of an X-ray data set from a Gre2p–$NADP^+$ crystal.

Values in parentheses are for the last shell.

Wavelength of data collection (Å)	0.91841
Resolution range (Å)	35.0–3.20 (3.28–3.20)
Space group	$P2_1$
Unit-cell parameters (Å, °)	$a = 60.54$, $b = 71.54$, $c = 77.98$, $\alpha = \gamma = 90$, $\beta = 104.49$
No. of measured reflections	55409
No. of unique reflections	10530
Unit-cell volume ($Å^3$)	3.23×10^5
Completeness (%)	97.5 (92.9)
$\langle I/\sigma(I)\rangle$	10.4 (2.4)
R_{merge}† (%)	17.0 (63.7)

† $R_{merge} = \sum_{hkl}\sum_i |I_i(hkl) - \langle I(hkl)\rangle| / \sum_{hkl}\sum_i I_i(hkl)$.

The Gre2p–$NADP^+$ crystals (Fig. 1) showed X-ray diffraction to a maximum resolution of 2.7 Å, but with a strongly anisotropic distribution (Fig. 2). A complete X-ray diffraction data set was collected and processed to 3.2 Å resolution (Table 1). Scaling and inspection of systematic absences revealed that the crystals belonged to space group $P2_1$. The overall quality of the diffraction data set was low and requires further optimization in order to solve the structure and to refine it to a satisfactory level.

We performed crystal-packing and noncrystallographic symmetry calculations based on the low-resolution data set documented in Table 1. On the basis of the unit-cell parameters, crystal symmetry and sequence length (342 amino acids), the program *MATTHEWS_COEF* (Collaborative Computational Project, Number 4, 1994) reported two Gre2p protomers per asymmetric unit as the most probable packing (probability 0.93), corresponding to a V_M value of 2.1 $Å^3\ Da^{-1}$ and a solvent content of 41.4%. The alternative solution with a probability of 0.06 and one protomer per asymmetric unit leads to a relatively high V_M value (4.2 $Å^3\ Da^{-1}$); however, the low diffraction quality of the crystals might be consistent with this.

For an unambiguous clarification of the number of Gre2p molecules per asymmetric unit, we performed Patterson search calculations. A native Patterson function was inconspicuous, *i.e.* no pseudo-origin peak could be detected. However, in a self-rotation calculation over the full rotation space ($0^\circ \le \varphi \le 180^\circ$, $0^\circ \le \psi \le 180^\circ$, $0^\circ \le \kappa \le 180^\circ$) using reflections from 15 to 3.5 Å resolution the highest noncrystallographic peaks were found on the $\kappa = 180^\circ$ section (peaks 1 and 1′ in Fig. 3). These two peaks have a signal-to-noise ratio of 6.5, which is 57.7% of that of the crystallographic twofold peak (peak 2 in Fig. 3), *i.e.* they are consistent with the existence of two Gre2p protomers per asymmetric unit. Either peak 1 or peak 1′ shows the rotation that maps the two protomers on each other, while the other is a Klug peak originating from the fact that the noncrystallographic dyad is perpendicular to the crystallographic dyad (peak 2 in Fig. 3).

The twofold symmetry between the two Gre2p protomers in the asymmetric unit is somewhat surprising since a dimeric quarternary structure of Gre2p has never been observed in solution. The structure solution, which is under way, will reveal the location and character of the dimerization interface.

We are grateful to the staff of the BESSY synchrotron, Berlin, Germany, for assistance during X-ray diffraction data collection.

References

Bradford, M. M. (1976). *Anal. Biochem.* **72**, 248–254.
Casamayor, A., Aldea, M., Casas, C., Herrero, E., Gamo, F. J., Lafuente, M. J., Gancedo, C. & Arino, J. (1995). *Yeast*, **11**, 1281–1288.

Chen, C. N., Porubleva, L., Shearer, G., Svrakic, M., Holden, L. G., Dover, J. L., Johnston, M., Chitnis, P. R. & Kohl, D. H. (2003). *Yeast*, **20**, 545–554.
Choi, Y., Choi, H., Kim, D., Uhm, K.-N. & Kim, H.-K. (2010). *Appl. Microbiol. Biotechnol.* **87**, 185–193.
Collaborative Computational Project, Number 4 (1994). *Acta Cryst.* D**50**, 760–763.
Ema, T., Ide, S., Okita, N. & Sakai, T. (2008). *Adv. Synth. Catal.* **350**, 2039–2044.
Ema, T., Moriya, H., Kofukuda, T., Ishida, T., Maehara, K., Utaka, M. & Sakai, T. (2001). *J. Org. Chem.* **66**, 8682–8684.
Filling, C., Berndt, K. D., Benach, J., Knapp, S., Prozorovski, T., Nordling, E., Ladenstein, R., Jornvall, H. & Oppermann, U. (2002). *J. Biol. Chem.* **277**, 25677–25684.
Garay-Arroyo, A. & Covarrubias, A. A. (1999). *Yeast*, **15**, 879–892.
Hauser, M., Horn, P., Tournu, H., Hauser, N. C., Hoheisel, J. D., Brown, A. J. P. & Dickinson, J. R. (2007). *FEMS Yeast Res.* **7**, 84–92.
Jörnvall, H., Persson, B., Krook, M., Atrian, S., Gonzalez-Duarte, R., Jeffery, J. & Ghosh, D. (1995). *Biochemistry*, **34**, 6003–6013.
Kabsch, W. (2010). *Acta Cryst.* D**66**, 125–132.
Kaluzna, I., Andrew, A. A., Bonilla, M., Martzen, M. R. & Stewart, J. D. (2002). *J. Mol. Catal. B Enzym.* **17**, 101–105.
Kamitori, S., Iguchi, A., Ohtaki, A., Yamada, M. & Kita, K. (2005). *J. Mol. Biol.* **352**, 551–558.
Laemmli, U. K. (1970). *Nature (London)*, **227**, 680–685.
Matthews, B. W. (1968). *J. Mol. Biol.* **33**, 491–497.
Müller, M., Katzberg, M., Bertau, M. & Hummel, W. (2010). *Org. Biomol. Chem.* **8**, 1540–1550.
Persson, B. *et al.* (2009). *Chem. Biol. Interact.* **178**, 94–98.
Tong, L. & Rossmann, M. (1997). *Methods Enzymol.* **276**, 594–611.
Vido, K., Spector, D., Lagniel, G., Lopez, S., Toledano, M. B. & Labarre, J. (2001). *J. Biol. Chem.* **276**, 8469–8474.
Warringer, J. & Blomberg, A. (2006). *Yeast*, **23**, 389–398.